Applied Surface Science 258 (2012) 3109–3114

Contents lists available at SciVerse ScienceDirect

Applied Surface Science

journal homepage: www.elsevier.com/locate/apsusc

Optical and structural properties of ZnO nanorods grown on graphene oxide and reduced graphene oxide film by hydrothermal method

U. Alver[a,*], W. Zhou[b,c], A.B. Belay[b,c], R. Krueger[b], K.O. Davis[b,c], N.S. Hickman[b,c]

[a] Department of Physics, Kahramanmaras Sutcu Imam University, K. Maras 46100, Turkey
[b] Nanoscience and Technology Center, University of Central Florida, Orlando, FL 32816, USA
[c] Florida Solar Energy Center, Cocoa, FL 32922, USA

ARTICLE INFO

Article history:
Received 6 May 2011
Received in revised form 4 August 2011
Accepted 11 November 2011
Available online 20 November 2011

Keywords:
ZnO nanorods
Graphene oxide
Hydrothermal
Seed layer

ABSTRACT

ZnO nanorods were grown on graphene oxide (GO) and reduced graphene oxide (RGO) films with seed layers by using simple hydrothermal method. The GO films were deposited by spray coating and then annealed at 400 °C in argon atmosphere to obtain RGO films. The optical and structural properties of the ZnO nanorods were systematically studied by scanning electron microscopy (SEM), X-ray diffraction (XRD) and ultraviolet-visible spectroscopy. The XRD patterns and SEM images show that without a seed layer, no ZnO nanorod deposition occurs on GO or RGO films. Transmittance of ZnO nanorods grown on RGO films was measured to be approximately 83% at 550 nm. Furthermore, while transmittance of RGO films increases with ZnO nanorod deposition, transmittance of GO decreases.

1. Introduction

In recent years, ZnO based nanostructures, such as nanorods, nanowires, nanobelts, and nanotubes have attracted a great research interest because of their scientific and technological applications [1–3]. ZnO is an n-type transparent semiconductor material with a wide direct band gap of 3.37 eV and a large exciton binding energy of 60 meV at room temperature. Moreover, it is stable upon exposure to high energy radiation and wet chemical etching [4]. These properties make ZnO a desirable material for many optoelectronic applications. ZnO nanostructured films can be fabricated by a hydrothermal method that is simple and inexpensive when compared to many of the other common deposition techniques such as thermal evaporation under vacuum and sputtering [5,6].

Another material, graphene, a single monolayer of graphite, has recently attracted tremendous attention due to its unique electrical and optical properties, since its discovery in 2004 [7–9]. Graphene has a very high carrier mobility and remarkable electroconductivity, mechanical flexibility, strong thermal/chemical stability and optical transparency [10–14]. A common low cost method to produce graphene is to first produce chemically modified graphene, such as graphene oxide (GO), and then reduce it by using chemical routes and temperature annealing [15,16]. Both GO and reduced GO (RGO) have potential application in optoelectronic devices, such as in organic light emitting diodes and organic solar cells as a transparent electrode material in place of indium thin oxide (ITO) [17–20] and in biology, for cellular imaging and drug delivery [21]. Graphene is much more flexible and less expensive than ITO and the work function of graphene (~4.6 eV) is very close to that of ITO (~4.8 eV) [22]. Various deposition methods have been used to grow graphene films, such as chemical vapor deposition (CVD) on a metal catalytic layer (Ni, Co) or on Cu [23,24], spin coating[25–28], and spray deposition [29,30]. Although CVD is the most successful one among these, a means of obtaining high quality graphene films, from graphite powder and its further reduction to graphene has been extensively studied due to its ease of fabrication and economic feasibility. In addition, in the electronics industry, graphene sheets on insulating substrates are a desirable configuration. The graphene thin films deposited by CVD on metals have to be transferred to insulating substrates, which is a difficult step. Spin coating is currently the dominant technique to fabricate GO films, but spray deposition is also receiving increased attention, particularly due to its improved compatibility with high-volume manufacturing environments. High transparency and low resistivity have been shown in spray-deposited GO films when compared to spin coating [29].

The growth of semiconductor nanocrystals on graphene layers is particularly interesting because nanostructures can offer additional functionality to graphene, such as high electrical conductivity, good optical transmittance and improved field emission and capacitive properties. Recently, Kim et al. [31] reported on the growth and photoluminescence characteristics of ZnO nanostructure layers

* Corresponding author.
E-mail address: alver@ksu.edu.tr (U. Alver).

0169-4332/$ – see front matter © 2011 Elsevier B.V. All rights reserved.
doi:10.1016/j.apsusc.2011.11.046

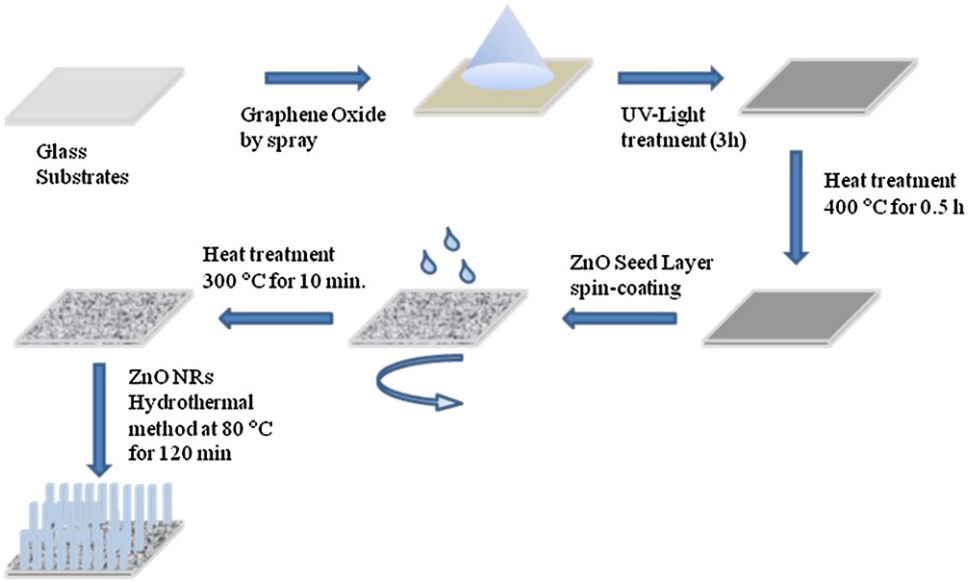

Fig. 1. A schematic illustration of ZnO nanorod grown on RGO and GO films.

on graphene layers using catalyst-free metal organic vapor-phase epitaxy. Hwang et al. [32] have presented the flexible field emission devices using hydrothermally growth of ZnO nanowires on reduced graphene/PDMS substrates. Yin et al. [33] have fabricated inorganic–organic hybrid solar cells with layered structure of quartz/RGO/ZnO NR/P3HT/PEDOT:PSS/Au, and observed a power conversion efficiency of 0.31%. While many other studies have been done on ZnO/graphene devices [34–38], so far no detailed study has been reported on the growth of ZnO nanorods (NRs) on graphene. Herein, we present results on the growth of ZnO NRs on GO and RGO films, with and without seed layers using a simple hydrothermal method. For comparison, results of ZnO NRs are also grown on seeded ITO (15 Ω/cm^2, 89.21% at 550 nm) and seeded bare glass substrate at 80 °C for 120 min are also presented.

2. Experimental

GO nanosheets were synthesized from natural graphite powder by Hummer's method [39]. In this work, 10 mg of GO powder was dispersed in 20 mL ethanol by ultrasonication for 3 h, forming a stable GO colloid. The glass substrates were initially cut to 2.5 cm × 2.5 cm and cleaned with deionized water (DI-water)-Triton-X100 mixture solution and ultrasonicated. The cleaning process was followed by rinses with actone and isoproponal, respectively, and then the substrates were dried in an oven at 100 °C. The cleaned glass substrates were further treated by UV/ozone exposure just before the spraying of GO.

GO films were deposited onto glass substrates by using a 2D airbrush spray coating system with pressurized nitrogen as the carrier gas and a substrate temperature set to 70 °C by a manually controlled heating unit. The spray nozzle-to-substrate distance was adjusted to 8.5 cm, and the lateral speed of the airbrush was set to 2 cm/s and the volumetric spray rate was set to approximately 3 μL/s by adjusting the nitrogen pressure. GO films were covered by quartz glass, then reduced by 3 h of exposure to UV radiation under a 40 W UV light [40]. Thermal reduction of GO films was carried out with 100 sccm flow of Ar gas at 400 °C in a quartz tube chamber from which the RGO films were obtained. Then, ZnO NRs were grown on RGO films in two steps, using the hydrothermal method, described by Guo et al. [41]. In the first step, RGO substrates were coated with a ZnO seed layer (SL) using a spin coating technique. The SL solution was prepared by dissolving 0.75 M zinc acetate dihydrate ($Zn(CH_3COO)_2{\cdot}2H_2O$) and 0.75 M ethanolamine ($NH_2CH_2CH_2OH$) in 2-methoxyethanol ($CH_3OCH_2CH_2OH$). The resulting mixture was stirred using a magnetic stirrer at 60 °C for 30 min to get a clear and stable coating solution. The RGO substrates were then spin-coated at 3000 rpm for 1 min. After spin coating, the samples were dried in air and then annealed in air at 300 °C for 10 min. The second step was to grow ZnO NRs on the seeded substrates using the hydrothermal method. The precursor solution was prepared by mixing an aqueous solution of 0.1 M zinc nitrate hexahydrate ($Zn(NO_3)_2{\cdot}2H_2O$) with 0.1 M hexamethylenetetramine ($C_6H_{12}N_4$) while keeping their volume ratio at 1:1. The seeded substrates were immersed in the precursor solution and suspended upside down in a sealed glass beaker. During the growth, the glass beaker was heated to 80 °C in a laboratory oven and maintained for 120 min without stirring. The substrates were removed from the beaker after reaction, and washed immediately in running DI water, and then dried in air before characterization. A schematic representation of ZnO NRs grown on GO and RGO films is shown in Fig. 1

Using a Digital Instrument, Nanoscope (R) IIIa in tapping mode, atomic force microscopy (AFM) measurements were carried out to characterize the surface of GO and RGO films. A Renishaw inVia Raman spectrometer was also used to analyze the effects of heat treatments on the crystal quality of graphene films. The optical transmission spectrum of the films was recorded using a Thermo Scientific Evolution 300, UV–vis spectrometer. The X-ray diffraction (XRD) measurements of the samples were performed on a Rigaku D/Max diffractometer with Cu Kα radiation to determine the structure of the films. The surface morphologies were observed using a Zeiss 55, field emission scanning electron microscope (FE-SEM).

3. Results and discussion

All of the GO films used in this study were prepared under identical deposition conditions. AFM images of GO and RGO films are shown in Fig. 2a and b. By using depth profile measurements of the films, the average thicknesses of the GO and RGO films were to be 8 nm and 11 nm, with corresponding rms roughness values of 3 nm and 5 nm, respectively. The overlapping GO sheets are clearly seen in Fig. 2a. GO films obtained on a glass surface showed a relatively smooth planar structure. The overall surface of the RGO thin films was also smooth, but exhibit a number of particle-like features on the surface as shown in Fig. 2b. These particle-like features might

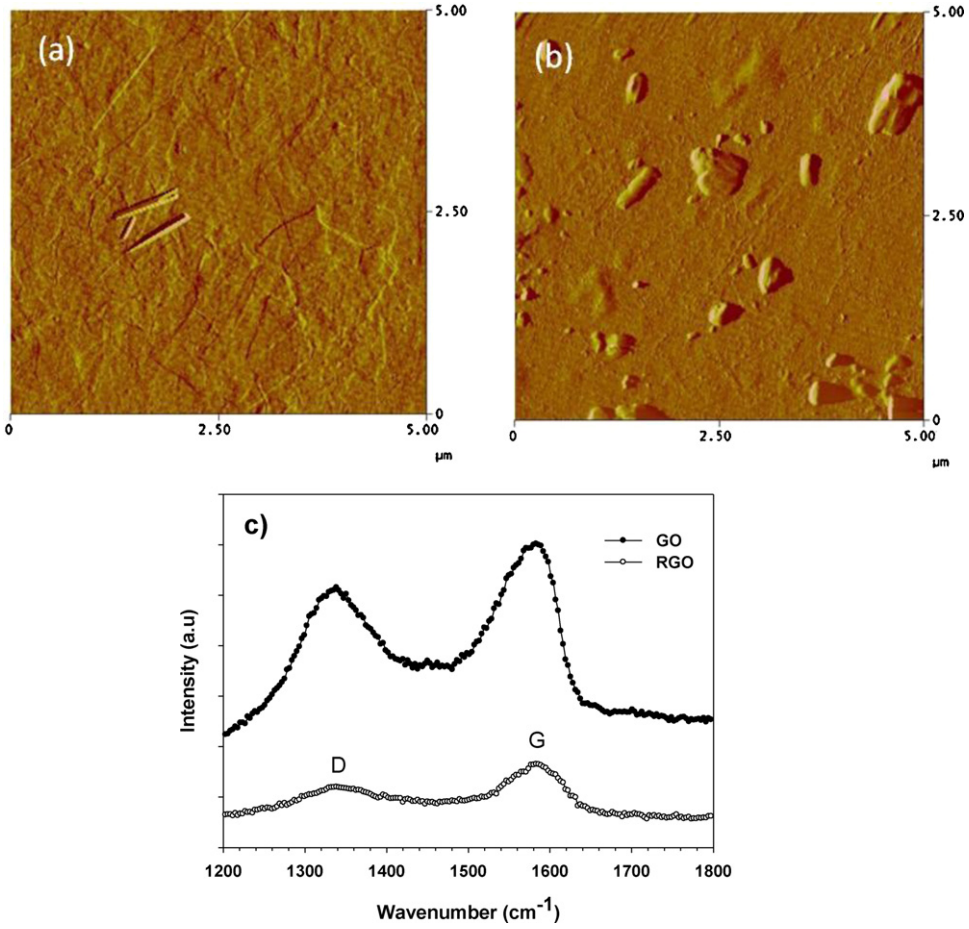

Fig. 2. AFM images and depth profile of GO/Glass (a), RGO/Glass films(b) and Raman spectra of GO and RGO (c).

arise due to aggregation of graphene sheets during annealing. GO is an electrically insulating material due to the presence of oxygen containing functional groups, such as epoxide, hydroxyl, carbonyl and carboxylic. After heat treatment, the color of GO films changed from the light brown to dark gray and the films became conductive. Raman measurements were also carried out for GO and RGO and the results are shown in Fig. 2c. As shown in Fig. 2c, the Raman spectra of GO films displays two prominent peaks at 1340 cm^{-1} (D bands) and at 1580 cm^{-1} (G bands), which are usually assigned to the breathing mode of κ-point phonons of A_{1g} symmetry and the E_{2g} phonon of C sp^2 atoms, respectively [42]. The prominent D peak is from the structural imperfections created by the attachment of hydroxyl and epoxide groups on the carbon basal plane. After UV and heat treatment, the magnitude of D band peak dropped, and the I_D/I_G ratio decreased from 0.755 to 0.708, showing a decreasing level of disorder carbon structure, which indicates a reduction of the GO film.

The sheet resistance of the RGO films, and the other samples were measured using a four-point probe method and the results are listed in Table 1. The resulting resistance values show that our GO films are partially reduced. The reason for the reduction in resistance can be explained by removing oxygen functional groups in the GO structure and decreasing the distance between graphene layers, creating continuous graphitic paths for charge transport [43].

Fig. 3 shows XRD patterns of ZnO NRs grown on different substrates at 80 °C for 120 min. The patterns of the ZnO NR array films deposited on bare glass, ITO, GO and RGO with a SL exhibit only one dominant peak, indexed as (0 0 2), corresponding to the ZnO wurtzite structure. This indicates that the ZnO NR arrays are well-oriented in the direction of the *c*-axis which is perpendicular to substrate surface. Such orientation of ZnO is an acceptable point, since the (0 0 2) plane of ZnO has the lowest surface energy [44] and the use of a spin coated SL has been shown to induce growth along the (0 0 2) direction [45]. The positions of the peaks and the other parameters related to the XRD results are listed in Table 1. However, no diffraction peaks assigned to ZnO are observed for the film ZnO/RGO/Glass films or the ZnO/GO/Glass films. The reason for this might be the low thickness of the films. The results indicate that the SLs have a great influence on ZnO nanorods growth. In addition, the full width at half maximum (FWHM) values of the (0 0 2) diffraction peaks, given in Table 1, reveal that grain size ZnO/SL/ITO are

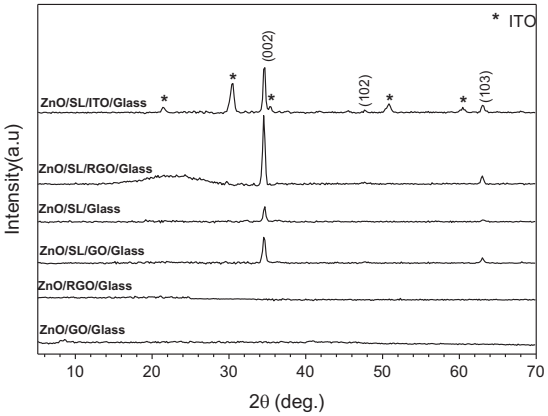

Fig. 3. XRD patterns of ZnO NRs on various substrates (Growth temperature: 80 °C for 120 min). The star indicates reflection from ITO substrate.

Table 1
Various parameters of ZnO films grown on different substrates.

Samples	Position of the (0 0 2) peaks (°)	*d* (nm)	FWHM (°)	Resistance (KΩ)
GO/Glass	–	–	–	–
RGO/Glass	–	–	–	900
ZnO/SL/ITO/Glass	34.612	2.5895	0.323	24
ZnO/SL/Glass	34.668	2.5854	0.343	184×10^3
ZnO/SL/RGO/Glass	34.585	2.5914	0.352	730
ZnO/SL/GO/Glass	34.603	2.5901	0.397	150×10^3

the smallest when compared to the others, since the FWHM value is inversely proportional to grain size of the films. No diffraction peaks were observed for GO and RGO films. Regarding the electrical properties, the resistance of ZnO/SL/RGO/Glass films was measured to be 730 kΩ which is less than RGO/glass film. This difference is likely due to either a highly oriented film for the ZnO/SL/RGO/Glass sample or to the formation of electrical path among RGO flakes through ZnO seed layers and highly conducting layers of ZnO nanorods and seed layers.

FE-SEM images of the ZnO NRs grown on different substrates are shown in Fig. 4(a–h). The thicknesses of the SLs and ZnO NRs are estimated to be 80 nm and 120 nm, respectively, from the cross sectional SEM images (Fig. 4h). The plane view of a SL with a diameter of 10–50 nm is given in Fig. 4c. In Fig. 4a and b, the ZnO NRs without

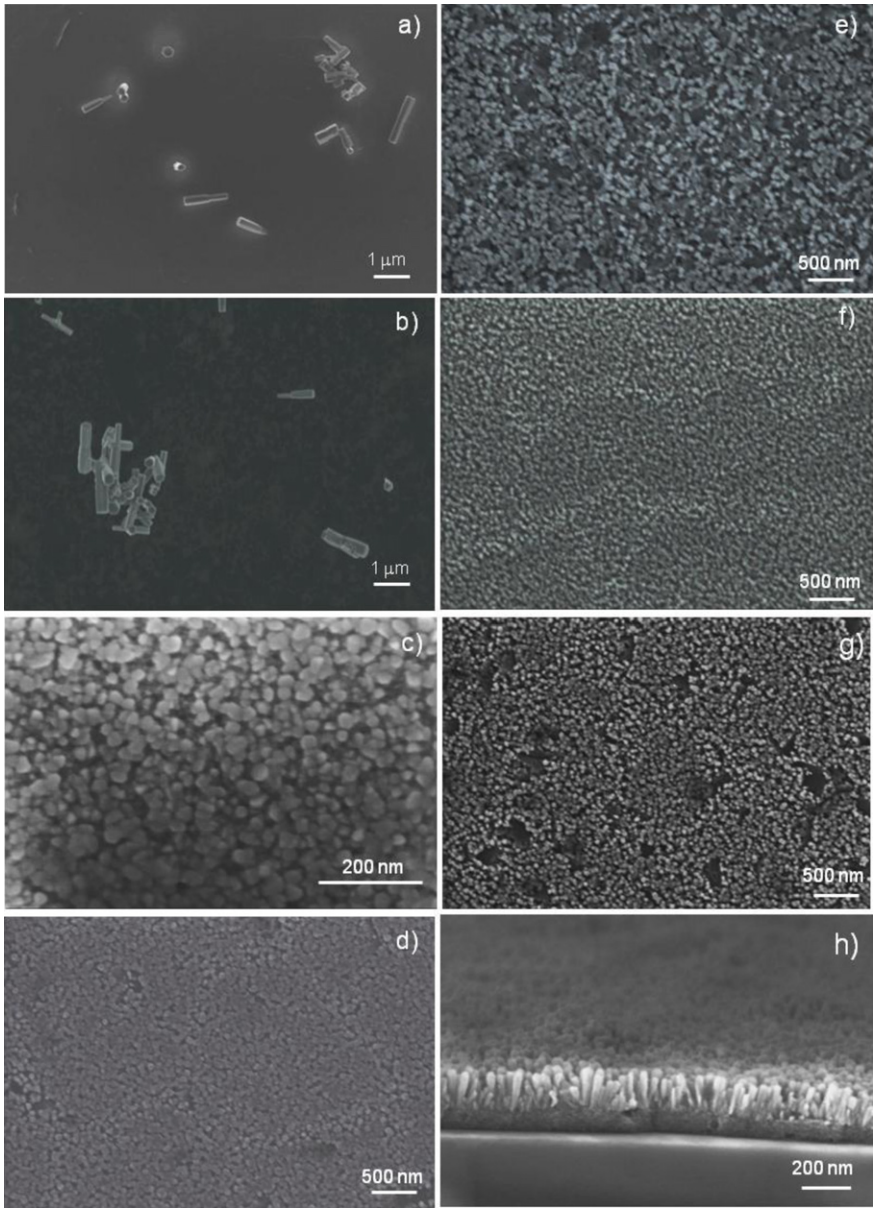

Fig. 4. SEM images of ZnO rods grown different substrates: (a) ZnO/GO/Glass; (b) ZnO/RGO/Glass; (c) SL/Glass; (d) ZnO/SL//Glass; (e) ZnO/SL/GO/Glass; (f) ZnO/SL/RGO/Glass; (g) ZnO/SL/ITO/Glass; (h) cross section of the ZnO/SL/RGO/Glass films.

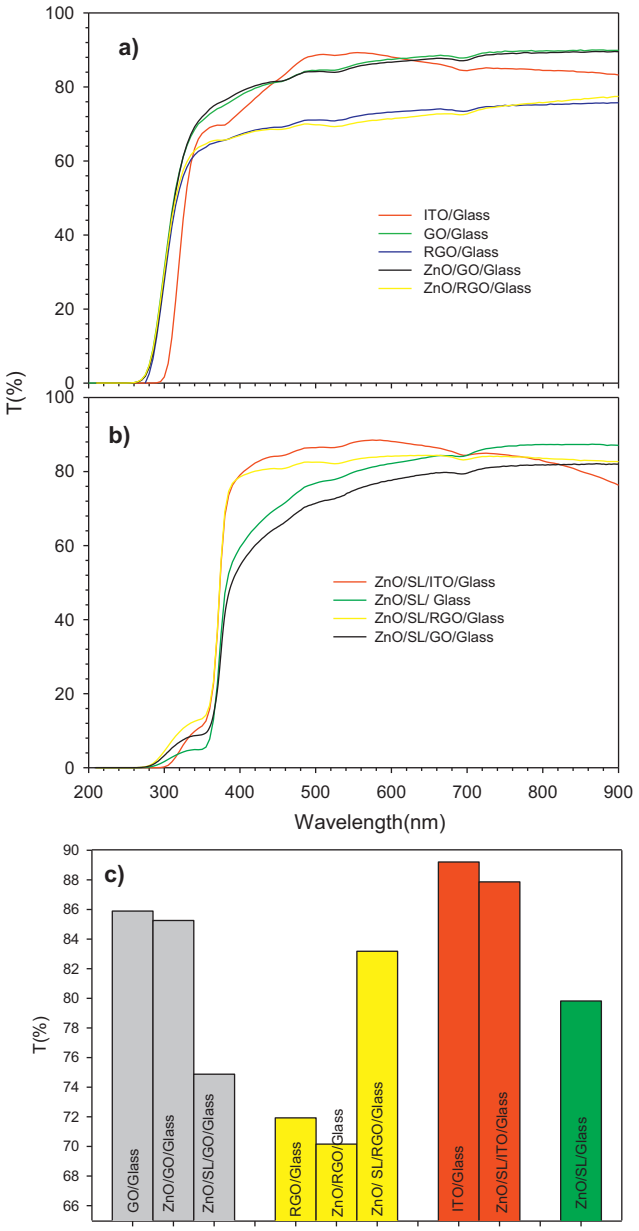

Fig. 5. UV–vis spectra of (a) GO, RGO, ZnO on GO and ZnO on RGO films without seed layer, (b) ZnO NR on seeded glass, ITO, GO and RGO at 80 °C for 120 min. (c) A bar graph of transmittances of the films at 550 nm.

a SLs are very limited in coverage and are randomly oriented on the GO and RGO films. This result supports the XRD results because no diffraction peaks assigned to ZnO nanorods were observed on the GO and RGO films. The reason for the poor crystallinity could be related to the rather large lattice mismatch between ZnO and GO or RGO. However, after depositing the SL on GO and RGO, dense, uniform and oriented films with an average diameter of 20–40 nm were obtained. This is an expected result because there is no lattice matching problem between ZnO and the modified surface. In addition to this, free energy barrier of activation for nucleation on the modified surface is lower than on that of the bare substrate. A similar result was obtained by Liu [46] where they deposited ZnO on GO film by immersing the seed coated GO films in a growth solution containing ammonia and zinc nitrate hexahydrate. They observed that the ZnO structure were scattered and randomly oriented on the GO films. But differing our results, they reported flower like ZnO structures on seeded GO films. The reason for this different structure might be the different preparation routes. As seen in the SEM images, for the ZnO/SL/RGO/Glass film (Fig. 4f), the surface is much smoother and more continuous and it is composed of uniform NRs of about 30 nm in diameter. However, for the other samples (Fig. 4d, e and g) the NRs distribution is not homogenous across the film surface. The ZnO/SL/GO/Glass and ZnO/SL/ITO/Glass samples exhibit a porous nanostructure when compared to the ZnO/SL/Glass and ZnO/SL/RGO/Glass samples.

The UV–vis transmission spectra for the ZnO rods grown on GO and RGO without a SL at 80 °C, for 120 min are shown in Fig. 5a. It is observed that the GO and RGO films exhibit a sharp absorption edge at approximately 275 nm. The optical transmittance of the GO and RGO films is measured to be over 78% and 65%, respectively, in the visible region. As seen in Fig. 5a, the optical transmittance spectra of ZnO/GO/Glass and ZnO/RGO/Glass is almost the same as that of GO/Glass and RGO/Glass. Consistent with the SEM and XRD results, the UV–vis results indicate that there is no significant ZnO growth on GO and RGO films.

Fig. 5b shows the transmittance spectra of ZnO rods grown on seeded substrates. As clearly seen in this figure, the SLs significantly change in the optical properties of the films. The sharp fall in transmittance at 380 nm, which shows the existence of ZnO rods, is observed for the ZnO/SL/RGO/Glass and ZnO/SL/ITO/Glass samples, but for the fall is much gradual for ZnO/SL/GO/Glass and ZnO/SL/Glass. In order to compare, the change in transmittance of the different samples at 550 nm, a bar graph is presented in Fig. 5c. The remarkable result, that is evident from Fig. 5c is that while the transmittance of ZnO nanorods grown on the SL/RGO/Glass substrate increases, the transmittance of ZnO nanorods grown on SL/GO/Glass and SL/ITO/Glass decreases. The reason for such a transmittance might be the crystallization quality of the ZnO thin films grown on those substrates. As seen in the SEM images (Fig. 5c–f), the most smooth and defect free surface is observed for the ZnO/SL/RGO/Glass sample (Fig. 5e). This leads to an increase of transmittance. The defects (holes) on the surfaces likely cause light scattering and accordingly decrease transmittance. In addition to that, the optical transmittance of the ZnO/SL/RGO/Glass (83.17% at 550 nm) is very close to that of ZnO/SL/ITO/Glass (87.86% at 550 nm). Such an optical transmittance of ZnO/SL/RGO/Glass is important in solar cell applications, because ZnO/SL/RGO/Glass can be used as an electrode in the inverted solar cell device architecture in place of ZnO/ITO.

4. Conclusions

Highly oriented ZnO nanorods were grown on GO and RGO films with a ZnO seed layer by a hydrothermal method at 80 °C for 120 min. The structure, morphology and optical properties of the ZnO nanorods on GO and RGO with and without seed layers were studied. Results showed that the ZnO nanorods grown on RGO films with a seed layer show the single (0 0 2) orientation much stronger than that of ZnO nanorods on GO. Additionally, ZnO nanorods on RGO with the seed layer have a continuous and smooth surface and higher optical transmittance than that of the GO. Growth does not occur on GO and RGO films without a seed layer. The results obtained from this study show that ZnO nanorods grown on RGO with a seed layer have a great potential application on various optoelectronic devices, particularly inverted organic solar cells by combining the excellent characteristics of graphene and optical characteristics of ZnO nanorods.

Acknowledgment

Financial support from The Scientific & Technological Research Council of Turkey (TUBITAK-BIDEB 2219) is gratefully acknowledged.

References

[1] M.H. Huang, S. Mao, H. Feick, H. Yan, Y. Wu, H. Kind, E. Weber, R. Russo, P. Yang, Room-temperature ultraviolet nanowire nanolasers, Science 292 (2001) 1897–1899.
[2] Z.L. Wang, Zinc oxide nanostructures: growth properties and applications, J. Phys. Condens. Matter 16 (2004) R829–R858.
[3] M. Law, L.E. Greene, J.C. Johnson, R. Saykally, P. Yang, Nanowire dye-sensitized solar cells, Nat. Mater. 4 (2005) 455–459.
[4] D.C. Look, Recent advances in ZnO materials and devices, Mater. Sci. Eng. B 80 (2001) 383–387.
[5] S. Naseem, M. Iqbal, K. Hussain, Optoelectrical and structural properties of evaporated indium oxide thin films, Sol. Energy Mater. Sol. Cells 31 (1993) 155–162.
[6] T.-H. Fang, S.-H. Kang, Surface and mechanical characteristics of ZnO:Al nanostructured films, J. Appl. Phys. 105 (2009) 113512.
[7] K.S. Novoselov, A.K. Geim, S.V. Morozov, D. Jiang, M.I. Katsnelson, I.V. Grigorieva, S.V. Dubonos, A.A. Firsov, Two-dimensional gas of massless Dirac fermions in graphene, Nature 438 (2005) 197–200.
[8] K.S. Novoselov, A.K. Geim, S.V. Morozov, D. Jiang, Y. Zhang, S.V. Dubonos, I.V. Grigorieva, A.A. Firsov, Electric Field Effect in Atomically Thin Carbon Films, Science 306 (2004) 666–669.
[9] R.R. Nair, P. Blake, A.N. Grigorenko, K.S. Novoselov, T.J. Booth, T. Stauber, N.M.R. Peres, A.K. Geim, Fine structure constant defines visual transparency of graphene, Science 320 (2008) 1308.
[10] G. Cravotto, P. Cintas, Sonication-assisted fabrication and post synthetic modification of graphene like materials, Chem. Eur. J. 16 (2010) 5246–5259.
[11] K.S. Kim, Y. Zhao, H. Jang, S.Y. Lee, J.M. Kim, J.H. Ahn, P. Kim, J.Y. Choi, B.H. Hong, Large-scale pattern growth of graphene films for stretchable transparent electrodes, Nature (London) 457 (2009) 706–710.
[12] G. Eda, G. Fanchini, M. Chhowalla, Large-area ultrathin films of reduced graphene oxide as a transparent and flexible electronic material, Nat. Nanotechnol. 3 (2008) 270–274.
[13] A.A. Balandin, S. Ghosh, W. Bao, I. Calizo, D. Teweldebrhan, F. Miao, C.N. Lau, Superior thermal conductivity of single-layer graphene, Nano Lett. 8 (2008) 902–907.
[14] X. Wang, L. Zhi, K. Mullen, Transparent, Conductive graphene electrodes for dye-sensitized solar cells, Nano Lett. 8 (2008) 323–327.
[15] S.J. Wang, Y. Geng, Q. Zheng, J.K. Kim, Fabrication of highly conducting and transparent graphene films, Carbon 48 (2010) 1815–1823.
[16] X. Zhou, X. Huang, X. Qi, S. Wu, C. Xue, F.Y.C. Boey, Q. Yan, P. Chen, H. Zhang, In situ synthesis of metal nanoparticles on single-layer graphene oxide and reduced graphene oxide surfaces, J. Phys. Chem. C 113 (2009) 10842–10846.
[17] T. Sun, Z.L. Wang, Z.J. Shi, G.Z. Ran, W.J. Xu, Z.Y. Wang, Y.Z. Li, L. Dai, G.G. Qin, Multilayered graphene used as anode of organic light emitting devices, Appl. Phys. Lett. 96 (2010) 133301.
[18] H. Park, J.A. Rowehl, K.K. Kim, V. Bulovic, J. Kong, Doped graphene electrodes for organic solar cells, Nanotechnology 21 (2010) 505204 (1–6).
[19] Y. Xu, G. Long, L. Huang, Y. Huang, X. Wan, Y. Ma, Y. Chen, Polymer photovoltaic devices with transparent graphene electrodes produced by spin-casting, Carbon 48 (2010) 3293–3311.
[20] Z.Y. Yin, S. Sun, T. Salim, S. Wu, X. Huang, Q. He, Y.M. Lam, H. Zhang, Organic photovoltaic devices using highly flexible reduced graphene oxide films as transparent electrodes, ACS Nano 4 (2010) 5263–5268.
[21] X. Sun, Z. Liu, K. Welsher, J.T. Robinson, A. Goodwin, S. Zaric, H. Dai, Nano-graphene oxide for cellular imaging and drug delivery, Nano Res. 1 (2008) 203–212.
[22] H. Hibino, H. Kageshima, M. Kotsugi, F. Maeda, F.Z. Guo, Y. Watanabe, Dependence of electronic properties of epitaxial few-layer graphene on the number of layers investigated by photoelectron emission microscopy, Phys. Rev. B 1 (2009) 79125437 (1–7).
[23] A. Reina, X. Jia, J. Ho, D. Nezich, H. Son, V. Bulovic, M.S. Dresselhaus, J. Kong, Large area few-layer graphene films on arbitrary substrates by chemical vapor deposition, Nano Lett. 9 (2009) 30–35.
[24] S. Bae, H. Kim, Y. Lee, X. Xu, J.-S. Park, Y. Zheng, J. Balakrishnan, T. Lei, H.R. Kim, Y. Il Song, Y.-J. Kim, K.S. Kim, B. Özyilmaz, J.-H. Ahn, B.H. Hong, S. Iijima, Roll-to-roll production of 30 in. graphene films for transparent electrodes, Nat. Nanotechnol. 5 (2010) 574–578.
[25] S. Watcharotone, D.A. Dikin, S. Stankovich, R. Piner, I. Jung, G.H.D. Dommett, G. Evmenenko, S.E. Wu, S.F. Chen, C.P. Liu, S.B.T. Nguyen, R.S. Ruoff, Graphene–silica composite thin films as transparent conductors, Nano Lett. 7 (2007) 1888–1892.
[26] B. Li, X. Cao, H.G. Ong, J.W. Cheah, X. Zhou, Z. Yin, H. Li, J. Wang, F. Boey, W. Huang, H. Zhang, All-carbon electronic devices fabricated by directly grown single-walled carbon nanotubes on reduced graphene oxide electrodes, Adv. Mater. 22 (2010) 3058–3061.
[27] J.Q. Liu, Z.Y. Yin, X.H. Cao, F. Zhao, A. Ling, L.H. Xie, Q.L. Fan, F. Boey, H. Zhang, W. Huang, Bulk heterojunction polymer memory devices with reduced graphene oxide as electrodes, ACS Nano 4 (2010) 3987–3992.
[28] S. Wu, Z. Yin, Q. He, G. Lu, X. Zhou, H. Zhang, Electrochemical deposition of Cl-doped n-type Cu_2O on reduced graphene oxide electrodes, J. Mater. Chem. 21 (2011) 3467–3470.
[29] P. Blake, P.D. Brimicombe, R.R. Nair, T.J. Booth, D. Jiang, F. Schedin, L.A. Ponomarenko, S.V. Morozov, H.F. Gleeson, E.W. Hill, A.K. Geim, K.S. Novoselov, Graphene-based liquid crystal device, Nano Lett. 8 (2008) 1704–1708.
[30] V.H. Pham, T.V. Cuong, S.H. Hur, E.W. Shin, J.S. Kim, J.S. Chung, E.J. Kim, Fast and simple fabrication of a large transparent chemically-converted graphene film by spray-coating, Carbon 48 (2010) 1945–1951.
[31] Y.J. Kim, J.H. Lee, G.C. Yi, Vertically aligned ZnO nanostructures grown on graphene layers, Appl. Phys. Lett. 95 (2009) 213101 (1–3).
[32] J.O. Hwang, D.H. Lee, J.Y. Kim, T.H. Han, B.H. Kim, M. Park, K. No, S.O. Kim, Vertical ZnO nanowires/graphene hybrids for transparent and flexible field emission, J. Mater. Chem. 21 (2011) 3432–3437.
[33] Z. Yin, S. Wu, X. Zhou, X. Huang, Q. Zhang, F. Boey, H. Zhang, Electrochemical deposition of Zno nanorods on transparent reduced graphene oxide electrodes for hybrid solar cells, Small 6 (2010) 307–312.
[34] Y. Zhang, H. Li, L. Pan, T. Lu, Z. Sun, Capacitive behavior of graphene–ZnO composite film for supercapacitors, J. Electroanal. Chem. 634 (2009) 68–71.
[35] W. Zou, J. Zhu, Y. Sun, X. Wang, Depositing ZnO nanoparticles onto graphene in a polyol system, Mater. Chem. Phys. 125 (2011) 617–620.
[36] W.T. Zheng, Y.M. Ho, H.W. Tian, M. Wen, J.L. Qi, Y.A. Li, Field emission from a composite of graphene sheets and ZnO nanowires, J. Phys. Chem. C 113 (2009) 9164–9168.
[37] J. Lin, M. Penchev, G. Wang, R.K. Paul, J. Zhong, X. Jing, M. Ozkan, C.S. Ozkan, Heterogeneous graphene nanostructures, ZnO nanostructures grown on large-area graphene layers, Small 6 (2010) 2448–2452.
[38] S. Wu, Z. Yin, Q. He, X. Huan, X. Zho, H. Zhang, Electrochemical deposition of semiconductor oxides on reduced graphene oxide-based flexible, transparent, and conductive electrodes, J. Phys. Chem. C 114 (2010) 11816–11821.
[39] W.S. Hummers, R.E. Offerman, Preparation of graphitic oxide, J. Am. Chem. Soc. 80 (1958) 1339.
[40] W. Zhou, A.B. Belay, R. Krueger, K. Davis, U. Alver, N.S. Hickman, Ultraviolet and thermal combined reduction of graphene oxide for application on transparent and conductive electrodes for solar cells, submitted for publication.
[41] M. Guo, P. Diao, X. Wang, S. Cai, The effect of hydrothermal growth temperature on preparation and photoelectrochemical performance of ZnO nanorod array films, J. Solid State Chem. 178 (2005) 3210–3215.
[42] A.C. Ferrari, J.C. Meyer, V. Scardaci, C. Casiraghi, M. Lazzeri, F. Mauri, S. Piscanec, D. Jiang, K.S. Novoselov, S. Roth, A.K. Geim, Raman spectrum of graphene and graphene layers, Phys. Rev. Lett. 97 (2006) 187401 (1–4).
[43] G. Lu, L.E. Ocola, J. Chen, Reduced graphene oxide for room-temperature gas sensors, Nanotechnology 20 (2009) 445502 (1–9).
[44] H.Z. Zhang, X.C. Sun, R.M. Wang, D.P. Yu, Growth and formation mechanism of c-oriented ZnO nanorod arrays deposited on glass, J. Cryst. Growth 269 (2004) 464–471.
[45] C. Zhang, High-quality oriented ZnO films grown by sol–gel process assisted with ZnO seed layer, J. Phys. Chem. Solids 71 (2010) 364–369.
[46] Y. Liu, G. Han, Y.M. Jin, Mater. Lett. (2011), 10.1016/j.matlet.2011.03.097.